I. ASL Kinetic Models

A. General Kinetic Model

Arterial spin labeling (ASL) is a magnetic resonance imaging (MRI) technique designed for quantifying absolute cerebral blood flow (CBF) values. In ASL MRI, the relationship between signal and perfusion parameter can be modeled as a mathematical formula based on the theory of tracer kinetics. The most common model currently used for ASL perfusion quantification is the general kinetic model which was originally proposed by Buxton et.al. [1]. The expression of label-control difference ΔM can be derived as equation (16):

$$= \begin{cases} 0, t < \Delta t \\ C(f, \Delta t) * \left(1 - e^{-(t-\Delta t)/T_{1\text{app}}}\right), \Delta t \leq t < \Delta t + \tau \\ C(f, \Delta t) * e^{-(t-\Delta t-\tau)/T_{1\text{app}}} \left(1 - e^{-\tau/T_{1\text{app}}}\right), \Delta t + \tau \leq t \end{cases} \tag{16}$$

where $C(f, \Delta t) = 2M_{0a} f T_{1\text{app}} e^{-\Delta t/T_{1b}}$ and $1/T_{\text{1app}} = 1/T_1 + f/\lambda$. Here f is the perfusion parameter, Δt is the arterial transit time (ATT), T_1 denotes the relaxation time of labeled blood in voxel, λ is the partition coefficient, M_{0a} denotes the total arterial magnetization, T_{1b} denotes the relaxation coefficient of arterial blood, τ represents the label duration and t is the inversion time.

B. Dispersion Kinetic Model

However, standard kinetic model is not perfect, a number of factors are not incorporated into it, for example, dispersion effects [2]. In general KM, a uniform plug flow is assumed as a way to deliver labeled blood to imaging region, but in practice because of the multiple confounding factors such as cardiac pulsatility and carotid bifurcation, blood bolus that are labeled at the same time may not arrive simultaneously. Dispersion effects are used to describe this. To incorporate dispersion effects into the original kinetic model, a modification is needed. The calculation of new dispersion kinetic model involves a multiplication between the original arterial input function and a scaling factor $s(t)$ [2]:

$$= \begin{cases} 0, t < \Delta t \\ 1 - Q(1 + sp, s(t - \Delta t)), \Delta t \leq t < \Delta t + \tau \\ Q(1 + sp, s(t - \Delta t - \tau)) - Q(1 + sp, s(t - \Delta t)), \Delta t + \tau \leq t \end{cases} \tag{17}$$

where $Q(x, y)$ is the incomplete gamma integral defined as:

$$Q(x, y) = \frac{1}{\Gamma(x)} \int_y^\infty e^{-t} t^{x-1} dt \tag{18}$$

where s and p are two parameters controlling the shape of dispersion. s denotes the sharpness and p denotes the time-to-peak. The zero time-to-peak and infinite sharpness refer to no dispersion.

II. Simulation Experiments

Figure 8 shows the error in estimated noise parameter from the simulation experiments across all methods and SNR. An overall consistency in error in estimated noise parameter was observed across the different inference frameworks on bi-exponential example and ASL forward models. The median errors in all experiments concentrated around zero or near to 0. Similar to other parameter of interest, larger errors can be observed at low SNR (wider inter-quartile range), except that the estimations by using aVB as inference algorithm and dispersion KM as the forward model exhibited a constant inter-quartile range.

III. Real Data Experiments

A. Real Data Experiment with Reduced Data Sets

Figure 9 shows the estimated perfusion and ATT using a reduced data with only one measurement at each PLD by using general KM (a) and dispersion KM (b) as the forward model. Similar to figure 7, perfusion was estimated with a clear pattern by using both VAE-like framework and the aVB analysis, however perfusion estimations appeared to be less smooth by using VAE-like framework. Similar to averaged data set, VAE-like framework still exhibited a longer ATT value in white matter, but it was less noticeable when using aVB.

B. Parameter Uncertainty

Figure 10 show the estimated parameter uncertainty (95% credible interval of the marginal posterior) from the real data experiment with an averaged data set as input data. Clear patterns of white and grey matter can be observed in each of the plots. The magnitude of uncertainty are similar between aVB inferred values and VAE inferred values except a smaller perfusion uncertainty by using aVB than VAE-like framework in both General KM and Dispersion KM.

Figure 11 show the estimated parameter uncertainty (95% credible interval of the marginal posterior) from the real data experiment with 8 reduced data sets as input data. The uncertainty of estimated perfusion by aVB was similar to VAE-like framework using both general KM and dispersion KM, while a larger uncertainty of ATT estimated by aVB using dispersion KM can be observed.

C. Noise Parameter

Figure 12 and 13 demonstrate the estimation of noise parameter from real data experiments using the average data set and reduced data sets respectively. In both cases, the noise parameter estimated by aVB is in similar magnitude with the one inferred by VAE-like framework, while aVB exhibited a better contrast between different types of tissues and VAE-like framework shows more constant estimations.

IV. Free Energy

Posterior probability distribution is often hard to be computed analytically because of intractable integrals. In this case, a simpler distribution $q(w)$ is often considered to approximate true posterior distribution $P(w|y)$. Free energy F is used to measure the difference between true and approximated posterior:

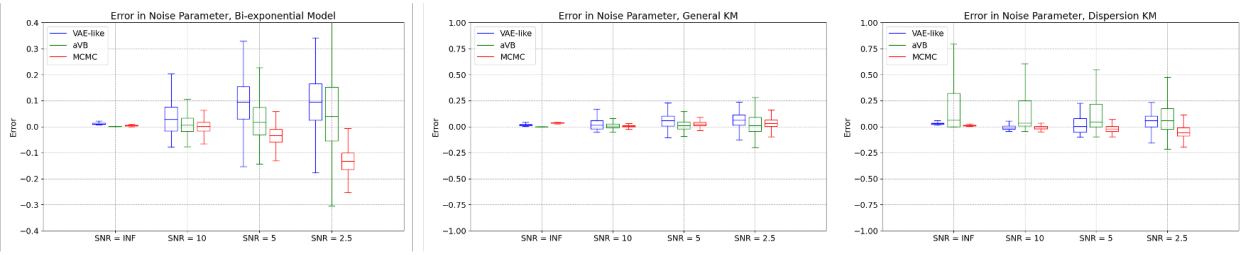

Fig. 8. Error in estimated noise parameter in simulation experiment:Three figures are noise parameter estimated by using bi-exponential model (Left), ASL General KM (Middle) and Dispersion KM (Right) as the forward model. In each experiment, aVB, MCMC and VAE-like framework were used as the inference algorithm.

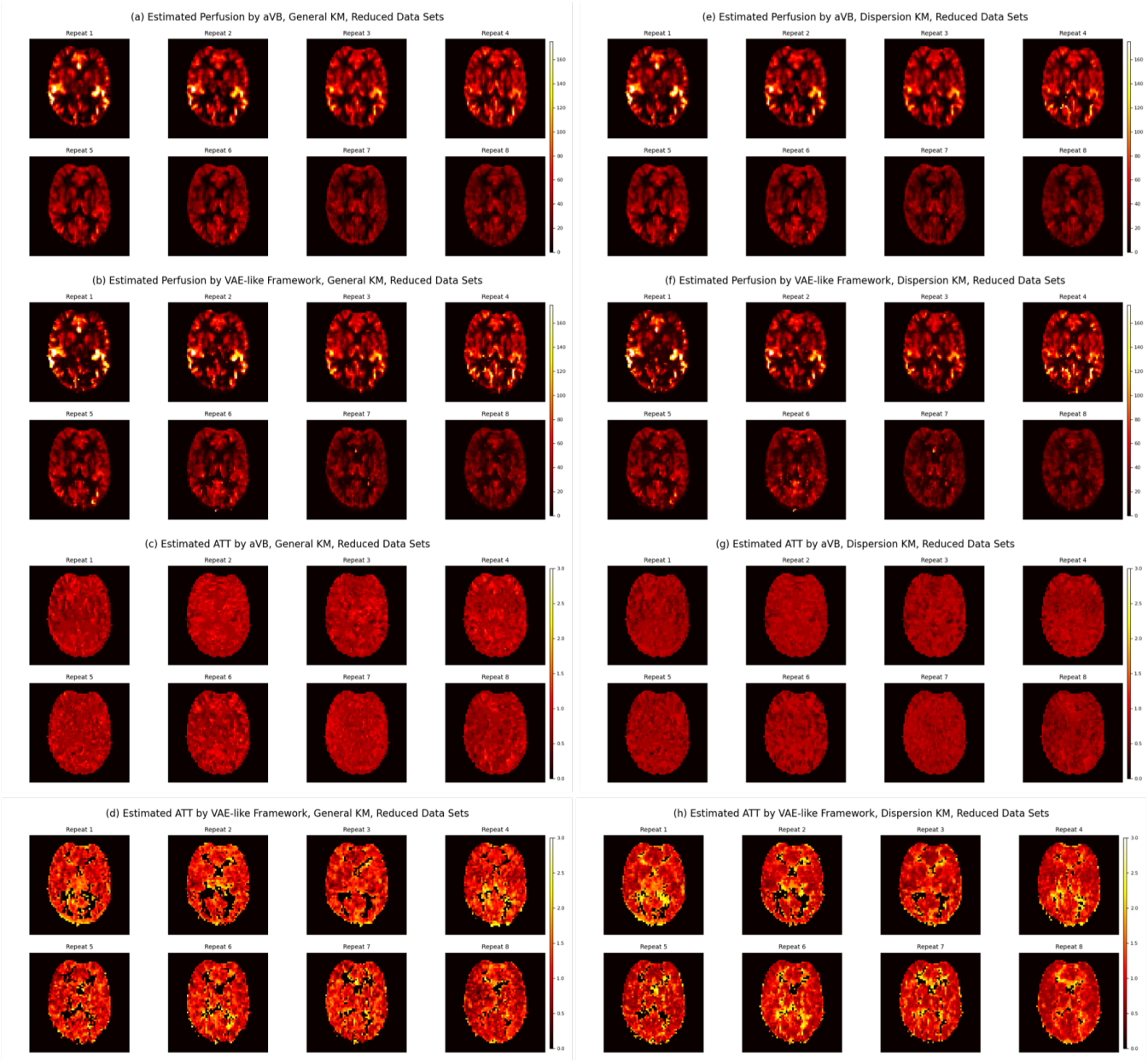

Fig. 9. Real Data Experiment with Reduced Data Sets: (a), (b), (c) and (d) are perfusion and ATT estimated with the General KM as the forward model; (e), (f), (g) and (h) are perfusion and ATT estimated with the General KM as the forward model; (a), (c), (e), (g) are inferred by using the aVB algorithm implemented in BASIL tool box; (b), (f), (d), (h) are inferred by using our VAE-like framework; Each figure contains the results from 8 single repeat. The brain mask used for ATT values was generated from perfusion greater than 5 ml/100g/min.

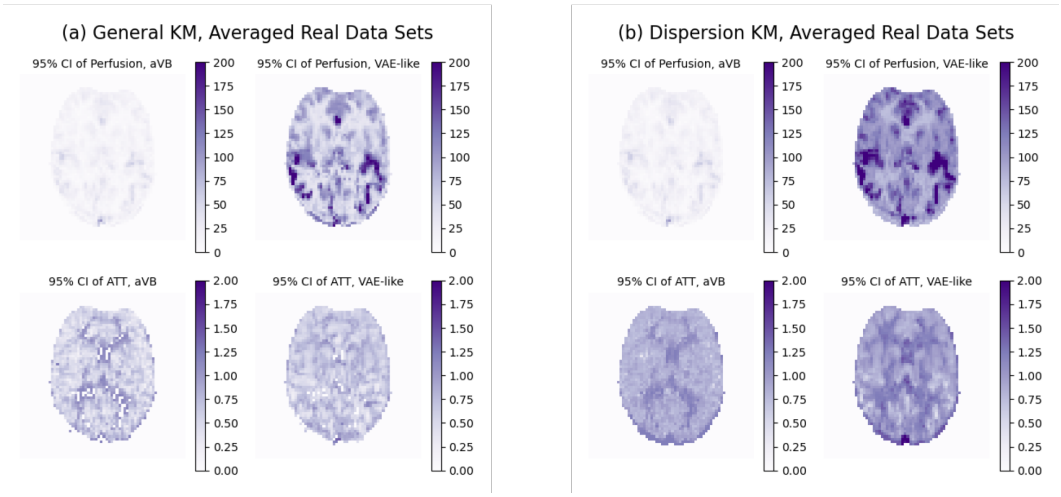

Fig. 10. Error in estimated noise parameter in simulation experiment:Three figures are noise parameter estimated by using bi-exponential model (Left), ASL General KM (Middle) and Dispersion KM (Right) as the forward model. In each experiment, aVB, MCMC and VAE-like framework were used as the inference algorithm.

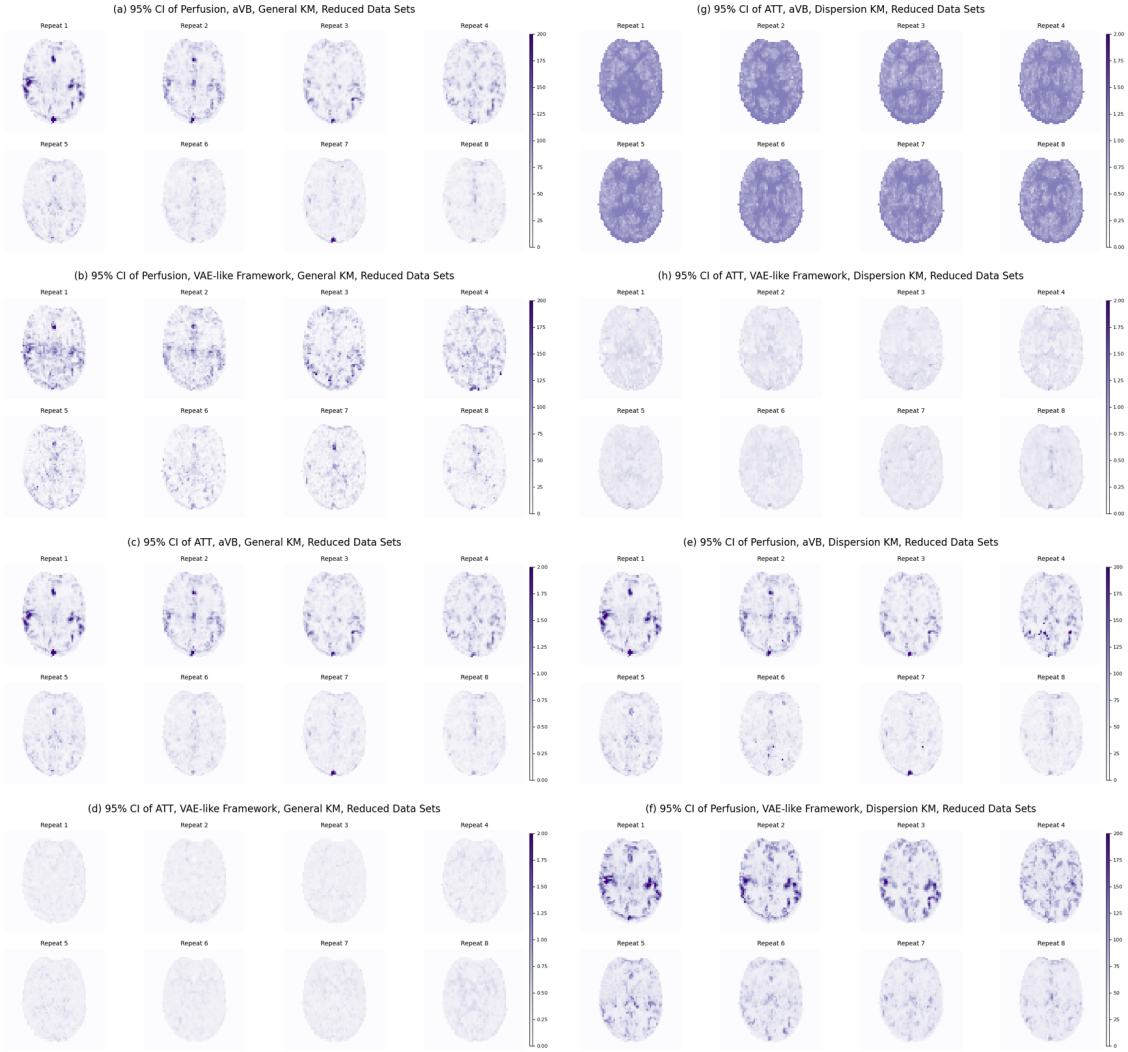

Fig. 11. Error in estimated noise parameter in simulation experiment:Three figures are noise parameter estimated by using bi-exponential model (Left), ASL General KM (Middle) and Dispersion KM (Right) as the forward model. In each experiment, aVB, MCMC and VAE-like framework were used as the inference algorithm.

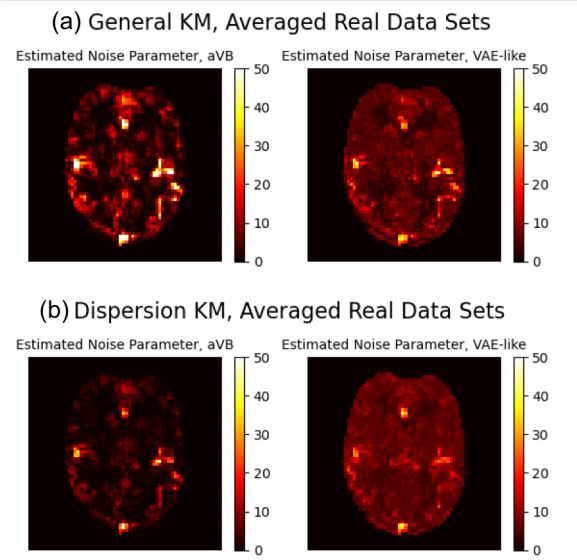

Fig. 12. Estimated Noise Parameter with Averaged Real Data Set: (a) by using general KM as the forward model; (b) by using dispersion KM as the forward model

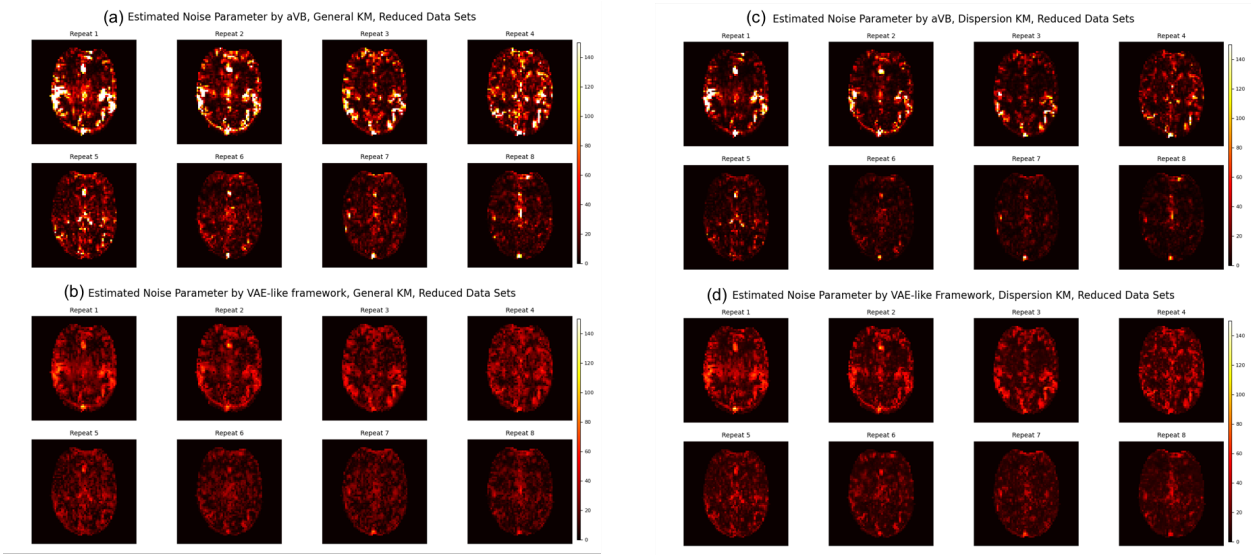

Fig. 13. Estimated Noise Parameter with Reduced Real Data Sets: (a)and (b) by using general KM as the forward model; (c) and (d) by using dispersion KM as the forward model; (a) and (c) are results estimated from aVB; (b) and (d) are results estimated from VAE-like framework;

$$F = \int q(\mathbf{w}) \log \left[\frac{P(\mathbf{y} \mid \mathbf{w}) P(\mathbf{w})}{q(\mathbf{w})} \right] d\mathbf{w} \tag{1}$$

By Jensen's inequality [3]:

$$\begin{aligned} F &= \textstyle\int q(\mathbf{w}) \log \left[\frac{P(\mathbf{y}|\mathbf{w}) P(\mathbf{w})}{q(\mathbf{w})} \right] d\mathbf{w} \\ &\leq \log \textstyle\int q(\mathbf{w}) \left[\frac{P(\mathbf{y}|\mathbf{w}) P(\mathbf{w})}{q(\mathbf{w})} \right] d\mathbf{w} \\ &= \log \textstyle\int P(\mathbf{y} \mid \mathbf{w}) P(\mathbf{w}) d\mathbf{w} \\ &= \log P(\mathbf{y}) \end{aligned} \tag{2}$$

where $F = logP(y)$ when $q(w) = P(w|y)$. Then finding the best estimate of true posterior is equivalent to the maximization of free energy F.

Moreover:

$$\begin{aligned} F &= \textstyle\int q(\mathbf{w}) \log \left[\frac{P(\mathbf{y}|\mathbf{w}) P(\mathbf{w})}{q(\mathbf{w})} \right] d\mathbf{w} \\ &= \textstyle\int q(\mathbf{w}) \log \left[\frac{P(\mathbf{y}|\mathbf{w}) P(\mathbf{w}|\mathbf{y}) P(\mathbf{w})}{q(\mathbf{w}) P(\mathbf{w}|\mathbf{y})} \right] d\mathbf{w} \\ &= \textstyle\int q(\mathbf{w}) \log \left[\frac{P(\mathbf{w}|\mathbf{y})}{q(\mathbf{w})} \cdot \frac{P(\mathbf{y}|\mathbf{w}) P(\mathbf{w})}{P(\mathbf{w}|\mathbf{y})} \right] d\mathbf{w} \\ &= \textstyle\int q(\mathbf{w}) \log P(\mathbf{y}) d\mathbf{w} - \int q(\mathbf{w}) \log \left[\frac{q(\mathbf{w})}{P(\mathbf{w}|\mathbf{y})} \right] d\mathbf{w} \\ &= \log P(\mathbf{y}) - KL[q(\mathbf{w}) \mid P(\mathbf{w} \mid \mathbf{y})] \end{aligned} \tag{3}$$

Thus the maximization of free energy is equivalent to the minimization of KL divergence. To achieve the best approximation of posterior, we can either maximize free energy or minimize the KL divergence.

REFERENCES

[1] Buxton, R B et al. "A general kinetic model for quantitative perfusion imaging with arterial spin labeling." *Magnetic resonance in medicine* vol. 40,3 (1998): 383-96. doi:10.1002/mrm.1910400308

[2] Chappell, Michael A et al. "Modeling dispersion in arterial spin labeling: validation using dynamic angiographic measurements." *Magnetic resonance in medicine* vol. 69,2 (2013): 563-70. doi:10.1002/mrm.24260

[3] Liao, J. G., Berg, Arthur,Sharpening Jensen's Inequality, Statistics Theory (math.ST)